
This is an electronic reprint of the original article.
This reprint may differ from the original in pagination and typographic detail.

Kätsyri, Jari; de Gelder, Beatrice; de Borst, Aline W.

Amygdala responds to direct gaze in real but not in computer-generated faces

Published in:
NeuroImage

DOI:
[10.1016/j.neuroimage.2019.116216](https://doi.org/10.1016/j.neuroimage.2019.116216)

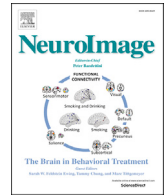
Published: 01/01/2020

Document Version
Publisher's PDF, also known as Version of record

Published under the following license:
CC BY-NC-ND

Please cite the original version:
Kätsyri, J., de Gelder, B., & de Borst, A. W. (2020). Amygdala responds to direct gaze in real but not in computer-generated faces. *NeuroImage*, 204, Article 116216. <https://doi.org/10.1016/j.neuroimage.2019.116216>

This material is protected by copyright and other intellectual property rights, and duplication or sale of all or part of any of the repository collections is not permitted, except that material may be duplicated by you for your research use or educational purposes in electronic or print form. You must obtain permission for any other use. Electronic or print copies may not be offered, whether for sale or otherwise to anyone who is not an authorised user.



Amygdala responds to direct gaze in real but not in computer-generated faces

Jari Kätsyri^{a,b,*}, Beatrice de Gelder^{a,c}, Aline W. de Borst^d

^a Brain and Emotion Laboratory, Department of Cognitive Neuroscience, Faculty of Psychology and Neuroscience, Maastricht University, Maastricht, the Netherlands

^b Department of Computer Science, Aalto University, Espoo, Finland

^c Department of Computer Science, University College London, London, United Kingdom

^d UCL Interaction Centre, University College London, London, United Kingdom

ABSTRACT

Computer-generated (CG) faces are an important visual interface for human-computer interaction in social contexts. Here we investigated whether the human brain processes emotion and gaze similarly in real and carefully matched CG faces. Real faces evoked greater responses in the fusiform face area than CG faces, particularly for fearful expressions. Emotional (angry and fearful) facial expressions evoked similar activations in the amygdala in real and CG faces. Direct as compared with averted gaze elicited greater fMRI responses in the amygdala regardless of facial expression but only for real and not for CG faces. We observed an interaction effect between gaze and emotion (i.e., the shared signal effect) in the right posterior temporal sulcus and other regions, but not in the amygdala, and we found no evidence for different shared signal effects in real and CG faces. Taken together, the present findings highlight similarities (emotional processing in the amygdala) and differences (overall processing in the fusiform face area, gaze processing in the amygdala) in the neural processing of real and CG faces.

1. Introduction

Realistic computer-generated (CG) face stimuli are now widely available for studying the perception of emotions and other social cues from the face. Computer animation models are a popular choice in studying facial expressions, as they allow generating research stimuli in ways that would not be possible with human actors (e.g., Jack et al., 2012). Some CG emotional facial expressions can also trigger physiological responses that are as intense as those of real human faces (e.g., Joyal, 2014). At the same time, most CG face models are still easily recognizable as human-made, especially when they are trying to express emotional or other social cues, which indicates that their neural processing likely diverges from real faces in the early perceptual phases. Whether CG faces are viable stimuli for research purposes hinges on whether they can tap into the same social and emotional neural processes as real human faces. Neural processing of social cues from real and CG faces has still received scarce research attention, even though it has important implications for research and human computer interaction. In the present investigation, we aim to uncover whether neural processing of real and carefully matched CG faces diverges, focusing on two social cues: gaze and emotion.

Face perception is sustained by a distributed and interconnected neural system (Fox et al., 2009; Haxby et al., 2000; Ishai et al., 2005;

Rossion et al., 2012; Vuilleumier and Pourtois, 2007). The lateral fusiform gyrus (FG), often termed as the fusiform face area (FFA), is often considered the major entry node into this network (e.g., Ishai, 2008). According to Haxby's model (Haxby et al., 2000; see also Iidaka, 2014), the inferior occipital gyrus (IOG; or the occipital face area, OFA) encodes low-level visual features of faces and provides input to the FFA for encoding invariant facial features (e.g., identity) and to the pSTS for encoding variant aspects of faces (e.g., gaze direction and facial expressions). Furthermore, Haxby's model posits that several other extended regions function in concert with these core regions to extract meaning from faces. In particular, the amygdala (AMG) can interact with core systems with respect to processing emotional and threat-related information (e.g., Mattavelli et al., 2014).

Given its focal role in integrating facial information and encoding invariant facial features, the FFA is a likely candidate for detecting quantitative differences between real and CG faces. Previous electroencephalography (EEG) studies have demonstrated weaker face-specific N170 responses over occipital-parietal areas for faces with decreasing realism (with the exception of neonatal stylizations; Schindler et al., 2017) and for robot as compared with human faces (Dubal et al., 2011), which provides indirect evidence for realism-related encoding in the FFA. In contrast to previous EEG studies, fMRI studies have provided inconsistent findings on the involvement of the FFA in distinguishing real

* Corresponding author. Brain and Emotion Laboratory, Department of Cognitive Neuroscience, Faculty of Psychology and Neuroscience, Maastricht University, Maastricht, the Netherlands.

E-mail address: jari.katsyri@aalto.fi (J. Kätsyri).

<https://doi.org/10.1016/j.neuroimage.2019.116216>

Received 30 April 2019; Received in revised form 22 August 2019; Accepted 19 September 2019

Available online 22 September 2019

1053-8119/© 2019 The Authors. Published by Elsevier Inc. This is an open access article under the CC BY-NC-ND license (<http://creativecommons.org/licenses/by-nc-nd/4.0/>).

and artificial faces: James et al. (2015) observed greater responses to real as compared with cartoon faces, whereas Tong et al. (2000) found no evidence for such differences. Assuming that near-human artificial entities can elicit aversive and even eerie feelings in their observers, as suggested by the uncanny valley hypothesis (Mori, 1970/2012), it is conceivable that CG faces would also evoke greater threat-related responses in the AMG than real faces. Hence, our first research question (Q1) was whether real and CG faces, irrespective of facial expression, are processed differently in the face perception network (the FFA and AMG in particular).

Given that the FFA and AMG are both involved in encoding emotions from human faces (e.g., Fusar-Poli et al., 2009), it is also reasonable to ask whether emotional facial expressions of real as compared with CG faces would evoke greater responses in these regions. Previous fMRI studies using robot faces as research stimuli have found mixed results for the FFA. Gobbini et al. (2011) showed that emotional facial expressions posed by a robot and a real human evoke similar responses in core face perception regions (the OFA, FFA, and STS), whereas Chaminade et al. (2010) observed greater responses to a robot's facial expressions in the FFA and occipital regions. Several fMRI studies have already employed CG facial expressions of emotion in lieu of real ones; as one example, Said (2010) investigated categorical and non-categorical responses in the pSTS using CG faces displaying morphs between anger and fear. To the best of our knowledge, to date only one fMRI study has yet explicitly compared real and CG facial expressions with each other. In this study, Moser et al. (2007) tentatively showed ($p < 0.05$, uncorrected) that CG as compared with real facial expressions elicit weaker responses in the FG, STS, and OMPFC but, importantly, similar activations in the AMG. However, their results were pooled across all basic emotions, which begs the question of whether different AMG responses to real and CG faces could be evoked by specific facial expressions. In the present study, we focused specifically on anger and fear, given that previous evidence indicates that the AMG is more sensitive to fear (Costafreda et al., 2008; Fusar-Poli et al., 2009) and possibly to anger (Mattavelli et al., 2014) than to other basic emotions. In our second research question (Q2), we hence asked whether emotional facial expressions of real as compared with CG faces would evoke different responses in the FFA and AMG.

Besides facial expression, gaze direction is arguably one of the most important social signals conveyed by the face. Previously, single-unit recordings in the macaque monkey have identified AMG cells that are sensitive to direct gaze (Brothers and Ring, 1993). Faces with direct as compared with averted gaze have consistently evoked greater AMG responses in PET (Calder et al., 2002; Kawashima et al., 1999; however, see also Calder et al., 2002; Wicker et al., 1998) and in fMRI neuroimaging studies with human participants (Burra et al., 2013; however, see Engell and Haxby, 2007). One possibility is that the AMG, via a subcortical face processing route, mediates affective responses to being looked at by another person (de Gelder and Rouw, 2001; Johnson, 2005; Nummenmaa and Calder, 2009; Senju and Johnson, 2009; Tamietto and de Gelder, 2010). Interestingly, in an EEG study, Pönkänen et al. (2011) showed that direct as compared with averted gaze evokes greater face-sensitive responses when observing live faces but not when observing face images. This suggests that the neural processing of direct gaze could be mediated by the perceived animacy of faces. Hence, our third research question (Q3) was whether real as compared with CG faces with direct gaze would evoke different responses in the AMG.

Instead of evoking effects independently of each other, gaze direction and facial expression could also interact. In particular, according to the shared signal hypothesis, gaze direction can amplify threat signals conveyed by angry (threat from the observed person) and fearful (threat from environment) facial expressions (Adams et al., 2003). Anger is consistently recognized faster and rated as more intense when combined with direct gaze, whereas fear is recognized faster and rated as more intense when combined with averted gaze (e.g., Adams and Kleck, 2005, 2003; El Zein et al., 2015; Sander et al., 2007; however, see also Bindemann et al., 2008). In agreement with the AMG's role in threat

processing, anger appears to evoke greater responses in the AMG when paired with direct rather than averted gaze (Sato et al., 2004). Recent evidence also indicates that fear evokes greater AMG responses when paired with averted rather than direct gaze, but this pattern only occurs when faces are presented briefly and it is reversed at longer display times (Adams et al., 2012; van der Zwaag et al., 2012). Several previous studies using longer display times actually demonstrated the opposite pattern to the shared signal effect (Adams et al., 2003; Hadjikhani et al., 2008; Sauer et al., 2014; Straube et al., 2010). Using CG faces, N'Diaye et al. (2009) demonstrated the shared signal effect for angry and fearful facial expressions in the AMG and other face-sensitive regions (e.g., the IOG and the right FG). Previous studies have not yet compared the shared signal effect in real and CG faces, however. Hence, in our fourth research question (Q4), we asked whether real and CG faces would evoke different shared signal responses in the AMG.

2. Materials and methods

2.1. Participants

Twenty-one right-handed healthy volunteers participated in this study. One participant was excluded from the analyses due to excessive head motion, which left us with a total of 20 participants (10 females; mean age 23.9 years, age range 18–36 years). All participants had normal or corrected-to-normal vision and fulfilled the institute's MRI safety criteria. The study was performed in accordance with the Declaration of Helsinki, and all procedures followed the regulations of the Ethical Review Committee of Psychology and Neuroscience at Maastricht University.

2.2. Stimuli

Static images depicting real faces from ten individuals (five females) were selected from the Radboud Faces Database (Langner et al., 2010; actor identities 1, 2, 5, 9, 30, 32, 36, 37, 58, and 71). A professional computer artist (R. B.) created CG replicas of the face images with MakeHuman (<http://www.makehumancommunity.org>) and Blender (<https://www.blender.org>) tools. We used three different facial expressions for each actor: anger, fear, and neutral; and three different gaze directions for each facial expression: direct, averted to the left, and averted to the right. A total of 180 stimuli were hence used in the experiment (2 face types \times 10 actors \times 3 facial expressions \times 3 gaze directions). Given that gaze shifts based on image manipulation might have produced unnatural scleral reflections as well as unnatural iris and pupil shapes, we instead adopted the averted-gaze eye regions from other images in the Radboud database that showed the same facial expression as the target images. Except for the eye region, faces with direct and averted gaze were always identical.

An oval mask was used to crop out the hair and neck regions in all images. Face regions inside the spherical masks were then matched for global luminance, contrast, and color in YCbCr color space (similarly as in Farid and Bravo, 2012) using inhouse functions written in Matlab (version R2016a). Given the sensitivity of the AMG to eye whites (Whalen, 2004), eye region was additionally matched for local luminance and contrast (separately in sclera, pupil, and iris regions) using Matlab and Photoshop (version CS6). Local matching was carried out across individual actors to eliminate systematic differences between i) real and CG variants of the neutral, angry, and fearful faces; and ii) faces with direct, averted-left, and averted-right gaze. Final stimuli are illustrated in Fig. 1.

2.3. Stimulus validation

Two independent pretest studies were carried out via Qualtrics platform (<https://www.qualtrics.com>). In the first pretest, 18 participants were asked to categorize each facial expression (angry, fearful, happy, or



Fig. 1. Samples of computer-generated (upper row) and real faces (lower row) from one actor. From left to right: neutral face with gaze averted to the left, angry face with direct gaze, and fearful face with gaze averted to the right.

neutral) into one of seven categories (six basic emotions plus neutral) and to rate how intense each basic emotion appeared on each face using a visual scale ranging from 0 (not at all intense) to 100 (extremely intense). We also considered happy expressions in this early phase, given that they would have allowed us to compare gaze-dependent effects also in positive and negative approach-related emotions (i.e., joy and anger; cf. Adams and Kleck, 2003). Categorical responses were transformed to percentage-correct recognition rates. For emotion intensity ratings, we only considered ratings for target emotions out of the six basic emotions (e.g., only anger ratings for angry facial expressions). This was not possible for neutral facial expressions, given that “neutral emotion” was not rated separately. Instead, we defined the intensity of neutral faces as the greatest intensity rating given to any of the six basic emotions. In the second pretest, 17 participants rated the realism of each face using a semantic differential scale from -3 (extremely artificial) to 3 (extremely realistic). Participants were asked to provide realism ratings for eye, mouth, skin, nose, and “overall” regions; and these items were averaged for statistical analysis. Analyses were carried out using a repeated-measures ANOVA with facial expression and face type as within-subjects factors.

Recognition rates were above chance level ($1/7 = 14\%$) for all facial expressions in both real and CG faces ($T(17) > 8.54, p < .001$). Comparisons between real and CG faces are summarized in Table 1. Anger and fear were recognized significantly more accurately from CG than from real faces, and anger also received higher intensity ratings in CG faces. In contrast, happy facial expressions were recognized less accurately and received lower intensity ratings in CG faces. As expected, all CG facial expressions received lower realism ratings than real faces. Taken together, pretest results verified that anger, fear, and neutral emotions were recognized at least as accurately from CG than from real faces, and that CG faces were judged as less realistic than real faces. Happy facial expressions, which were recognized poorly from CG faces, were dropped from the present investigation.

Table 1
Pretest validation results for CG stimuli.

Rating	Real	CG	Diff. ^a	SE	
Recognition					
Anger	81%	97%	16%	4%	***
Fear	55%	74%	19%	5%	**
Happiness	98%	81%	-17%	6%	***
Neutral	74%	80%	6%	3%	
Intensity					
Anger	62.5	69.9	7.4	3.2	*
Fear	57.3	61.9	4.7	3.2	
Happiness	74.4	44.6	-29.8	3.6	***
Neutral	15.3	12.5	2.8	1.4	
Realism					
Anger	1.9	-2.3	-4.1	0.2	***
Fear	1.7	-2.4	-4.2	0.2	***
Neutral	1.7	-1.2	-2.9	0.2	***

Note. * $p < .05$. ** $p < .01$. *** $p < .001$.

^a Difference between CG and real faces.

2.4. Procedure and tasks

At the start of the session, participants were informed about the study, filled out the MRI safety checklist, signed the informed consent form, and received task instructions.

2.4.1. Functional MRI main task

The fMRI experiment consisted of three functional runs of the main task, one functional run of the face-localizer task, and one anatomical run. The fMRI task employed a block design with three factors: Face type (REAL, CG), facial expression (anger [ANG], fear [FEA], neutral [NTR]), and gaze direction (direct [DIR], averted [AVT]). These 12 stimulation blocks were repeated twice in each functional run in a random order. For AVT blocks, one of the repetitions always had gaze averted to the left, while the other one had gaze averted to the right. Following previous

findings showing that the shared signal hypothesis only occurs for briefly presented stimuli (Adams et al., 2012; van der Zwaag et al., 2012), stimuli within each block were displayed for 300 ms. Stimuli were presented in a random order and separated by a 1200-ms inter-stimulus interval. Each 15-s block was followed by a 15-s period of rest. Stimuli were presented on a uniform grey background and overlaid with a white crosshair, which also remained visible during the rest periods.

Within each block, one randomly chosen trial served as a catch trial. For these catch trials, a red circle surrounded the crosshair and remained visible on top of the face image for the duration of the stimulus. Participants were instructed to fixate on the crosshair and to press a button with their right index finger as fast and as accurately as possible whenever they detected the circle. This catch trial task was intended to keep participants alert throughout the experiment and to reduce conscious thought processes related to the experimental manipulation.

The experiment was performed using Presentation software (Version 20.0, Neurobehavioral Systems, Inc., Berkeley, CA, www.neurobs.com). Stimuli were back-projected onto a screen (width = 40 cm; height = 24.5; diagonal = 47 cm; resolution = 1920 × 1200) situated at the posterior end of the scanner bore. Participants viewed the stimuli through a mirror attached to the head coil (eye–screen distance approximately 75 cm). Images were displayed at a resolution of 246 × 328 (visual angle 3.9 × 5.1°).

2.4.2. Functional MRI localizer task

Participants viewed static black-and-white images of faces and houses adopted from a previous localizer study (Engelen et al., 2015). Eight blocks of faces and eight blocks of houses were presented in an AB design. Within each block, twelve images of different faces (six females) or twelve images of different houses were shown in a random order for 800 ms each and with a 200 ms inter-stimulus interval. Each 12-s block was followed by a 12-s period of rest. All stimuli were presented on a uniform grey background and overlaid with a white crosshair, which remained visible during the rest. Participants were instructed to fixate their gaze on the crosshair throughout the study. Images were displayed at a resolution of 252 × 252 (visual angle 4.0 × 3.9°).

2.4.3. Behavioral valence rating task

After the fMRI experiment, participants were led to a psychophysics lab adjacent to the scanner room, where they performed a behavioral rating task on a desktop PC. In this task, they rated the emotional valence of the same stimuli as used in the fMRI experiment by clicking on a visual scale with endpoints anchored at extreme unpleasantness (−100) to extreme pleasantness (100). Similarly as in the fMRI experiment, stimuli were presented for 300 ms. Given that the shared signal effect is stronger for subjective than for objective ratings (Sato et al., 2004), we explicitly instructed participants to rate their own subjective reactions to the stimuli. Averted gaze direction was assigned to the left for half of the actors and to the right for the other, and this assignment was counter-balanced across participants. Valence ratings were averaged across actors, standardized within-subjects to eliminate range effects, and analyzed using repeated-measures ANOVA.

2.5. Functional MRI data acquisition

A 3T Siemens MR scanner (MAGNETOM Prisma, Siemens Medical Systems, Erlangen, Germany) was used for imaging. Functional scans were acquired with a multiband gradient echo echo-planar imaging sequence with repetition time (TR) of 1500 ms and echo time (TE) of 30 ms. One extra volume was acquired at the beginning and end of each run. The three main functional runs consisted of 482 vol each and the functional localizer run consisted of 258 vol, each volume comprising 57 slices (matrix = 100 × 100, 2 mm isotropic voxels, inter-slice time = 26 ms, flip angle = 77°). High resolution T1-weighted structural brain images were acquired with an MPRAGE scan with a TR of 2250 ms and a TE of 2.21 ms, comprising of 192 slices (matrix = 256 × 256, 1 mm

isotropic voxels, flip angle = 9°).

2.6. Data analyses

2.6.1. Functional MRI pre-processing

The fMRI data were pre-processed, analyzed, and visualized using BrainVoyager software (Version 20.6; Brain Innovation B.V., Maastricht, the Netherlands). Functional data were corrected for head motion and slice scan time differences, temporally high-pass filtered (3 sines/cosines per run), and spatially smoothed using a Gaussian kernel (FWHM = 6 mm) except for localizer data that were not smoothed. Anatomical data were corrected for intensity inhomogeneity (Goebel et al., 2006) and transformed into MNI-152 space (ICBM; Fonov et al., 2011). The functional data were then aligned with the anatomical data and transformed into the same space to create 4D volume time-courses (VTCs).

2.6.2. Regions of interest

Following our *a priori* research questions, we defined regions-of-interest (ROI) bilaterally in the fusiform face area (FFA) and the amygdala (AMG), as summarized in Table 2 and illustrated in Fig. 2. We calculated single-subject General Linear Models (GLMs) and “Faces > Houses” contrast maps from the spatially unsmoothed separate localizer data of each participant. Following a previous recommendation for identifying individual ROIs (Kawabata Duncan and Devlin, 2011), we adopted a threshold of $p < .01$ (uncorrected) to identify face-sensitive regions in each subject. We restricted the size of ROI by only including voxels up to 10 mm from the peak voxel, and we only accepted activation clusters that were anatomically plausible and whose time courses resembled the HRF function. As a sanity check, we also verified that the individual FFA-ROIs were located close to the corresponding group-level FG activation loci for contrast “Faces > Houses” (cf. Jiang et al., 2009; Ramon et al., 2010; Schultz and Pilz, 2009). Using the described procedure, we were able to identify the bilateral FFA successfully in 18 out of 20 participants. Given that we were unable to identify the AMG even at a more lenient threshold of $p < .05$, bilateral AMG was instead annotated manually based on participants’ MNI transformed anatomical images. We carried out a manipulation check to ensure that these anatomically rather than functionally defined AMG-ROIs were sensitive to faces in the localizer data. Paired T-tests confirmed that the contrast “Faces > Houses” for mean beta values in these ROIs elicited significant positive responses with large effect sizes (left AMG: $M = 0.13$, $SE = 0.04$, $T(19) = 3.48$, $p = .003$, $d = 0.78$; right AMG: $M = 0.13$, $SE = 0.03$, $T(19) = 3.91$, $p < .001$, $d = 0.87$).

2.6.3. Planned contrasts

We used nine orthogonal contrasts to investigate our research questions. One contrast was used to test Q1: difference between real and CG faces (REAL > CG). Four contrasts were used to test main effects related to other research questions: for Q2, main effect of emotion (ANG + FEA > NTR) and the difference between fear and anger (FEA > ANG); for Q3, direct gaze effect (DIR > AVT); and for Q4, shared signal effect (DIR > AVT × ANG > FEA). Two contrasts were used to test Q2: different emotion-related effect in real and CG faces (REAL > CG × ANG + FEA > NTR) and different response to fear and anger in real and CG faces (REAL

Table 2

Mean coordinates (SDs in parentheses) for the FFA and AMG regions-of-interest as defined based on localizer and structural scans, respectively.

Region	Side	N	MNI coordinates			N. voxels
			x	y	z	
FFA	L	18	−40.6 (3.9)	−47.6 (6.5)	−19.5 (3.2)	212 (149)
	R	18	42.7 (2.5)	−47.6 (6.7)	−20.7 (2.5)	214 (140)
AMG	L	20	−22.2 (1.0)	−3.2 (0.9)	−21.0 (1.6)	2645 (467)
	R	20	23.4 (0.9)	−1.8 (0.9)	−20.9 (1.6)	2514 (315)

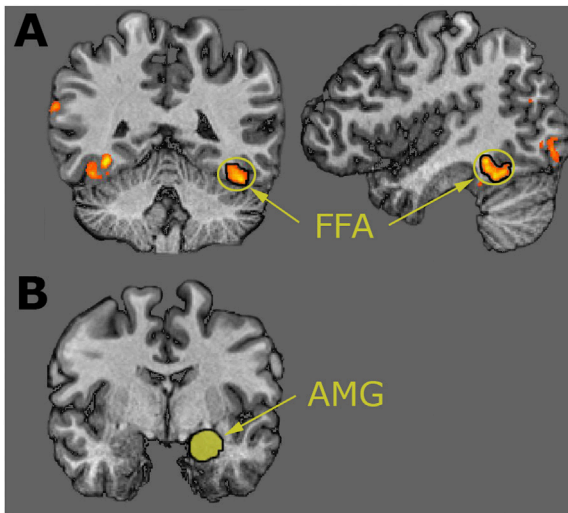


Fig. 2. Illustrations of regions-of-interest in the left hemisphere of one subject as defined based on a) face-localizer task and b) structural data. FFA – fusiform face area, AMG – amygdala.

> CG × FEA > ANG). Two contrasts were used to test Q3 and Q4: different direct-gaze effect in real and CG faces (REAL > CG × DIR > AVT) and different shared signal effect in real and CG faces (REAL > CG × DIR > AVT × ANG > FEA). When appropriate, simple effect tests were carried out separately for real and CG faces (e.g., DIR > AVT separately for real and CG faces).

2.6.4. Statistical analyses

For ROI analysis, weights for individual conditions were set according to planned contrasts and mean beta values were derived for each ROI accordingly. Statistical analyses were carried out using repeated-measures ANOVA with significance threshold set to $p < .05$ (two-tailed). A limitation of traditional null hypothesis significance testing is that it cannot provide support for the null hypothesis (Masson, 2011; Wagenmakers, 2007). To overcome this limitation in our ROI analysis, we estimated Bayesian posterior probabilities $P(H_0|D)$ and $P(H_1|D)$ for the null and alternative hypotheses based on the Bayesian Information Criteria following the guidelines of Masson (2011). Nominally, probability greater than or equal to .75 can be considered as positive evidence and probability greater than or equal to .95 as strong evidence for hypothesis H_1 (Masson, 2011; Raftery, 1999).

For the whole-brain analysis, a random-effects GLM analysis was carried out at the group level. Time courses of the 12 experimental

conditions were convolved with a two-gamma hemodynamic response function and included as predictors in the model, along with six z-transformed nuisance predictors for head translation and rotation parameters. For statistical significance testing, experimental predictors were subjected to random-effects analysis of variance with weights set according to planned contrasts. To correct for multiple comparisons, we used a cluster-level threshold procedure based on Monte Carlo simulation (Goebel et al., 2006) with an initial threshold $p < .001$, alpha level $p < .05$, and 1000 iterations. The anatomical locations of activated regions were labeled in accordance with the AAL atlas (Desikan et al., 2006). We also consulted common anatomical terms as identified by a lexical reverse-inference analysis carried out with NeuroSynth software (Yarkoni et al., 2011).

3. Results

3.1. Behavioral results

3.1.1. Valence ratings

As illustrated in Fig. 3, valence ratings were strongly influenced by facial expression and, to a lesser extent, face type. Angry and fearful faces were rated more unpleasant than neutral faces (contrast ANG + FEA > NTR; $F(1, 19) = 247.28, p < .001, \eta_p^2 = .93, P(H_1|D) > .99$). This difference was significantly greater for CG than for real faces (REAL > CG × ANG + FEA > NTR; $F(1, 19) = 5.13, p = .035, \eta_p^2 = .21, P(H_1|D) = .71$). All other planned contrasts were non-significant ($F_s \leq 2.91, p_s \geq .104, P(H_1|D) \leq .48$). In particular, Bayesian analysis suggested that the valence rating data were more in favor of the null hypothesis than either the shared signal hypothesis (DIR > AVT × ANG > FEA; $P(H_0|D) = .78$) or the direct gaze hypothesis (DIR > AVT; $P(H_0|D) = .81$).

3.1.2. Catch trial task performance

Performance in the catch trial task during fMRI scanning was close to ceiling (mean hit rate: range 94%–100%; mean false alarm rate: range 0%–7%). Consequently, six participants with 100% hit rate and two participants with 0% false alarm rate were excluded from corresponding analyses due to zero variance. Hit and false alarm rates were arcsine-transformed prior to analysis. Results indicated that target detection within blocks of real as compared with CG faces (REAL > CG) elicited lower hit rates ($M = 95\%$ and 99% ; $F(1, 13) = 15.56, p = .002, \eta_p^2 = .54, P(H_1|D) = .99$) and higher false alarm rates ($M = 4\%$ and 1% , $F(1, 17) = 9.85, p = .006, \eta_p^2 = .37, P(H_1|D) = .94$). No other planned contrasts were statistically significant ($F_s \leq 4.04, p_s \geq .061, P(H_1|D) \leq .62$).

3.1.3. Real versus CG faces

Our first research question was whether real and CG faces would elicit

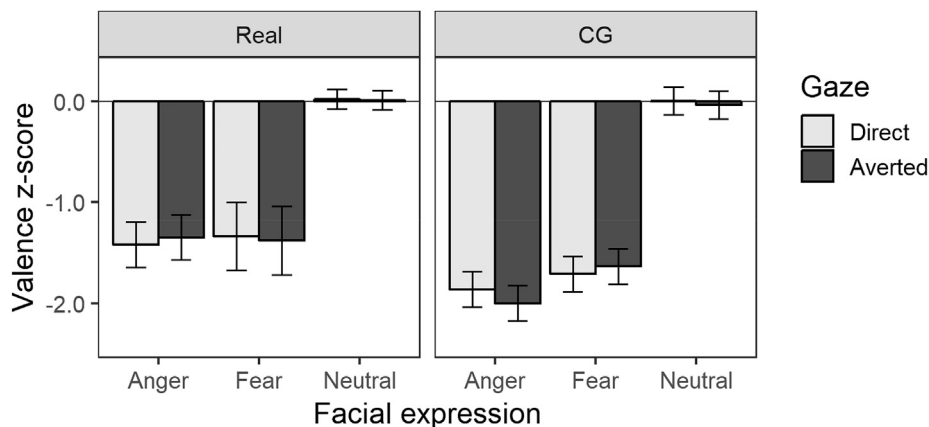


Fig. 3. Self-reported valence z-scores by face type, facial expression, and gaze direction. For visualization, data are centered at zero mean for neutral faces (grand-mean centered data were used in analysis). Error bars denote 95% CIs for difference between direct and averted gaze.

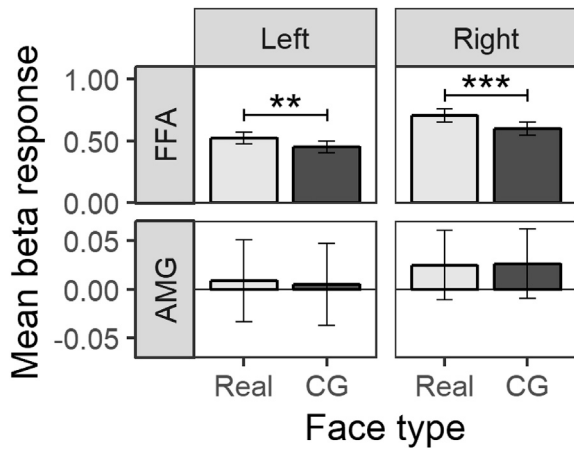


Fig. 4. Mean BOLD responses by face type in the left and right fusiform face area (FFA) and amygdala (AMG). Error bars denote 95% CIs for difference between real and CG faces, and asterisks denote significant differences (** $p < .01$, *** $p < .001$).

different responses in the FFA or AMG. As illustrated in Fig. 4, ROI analysis showed that real faces elicited significantly greater activations in the FFA (left: $F(1, 17) = 10.84, p = .004, \eta_p^2 = .40, P(H_1|D) = .95$; right: $F(1, 17) = 16.48, p < .001, \eta_p^2 = .49, P(H_1|D) = .99$) but not in the AMG (left: $F < 1, P(H_0|D) = .81$; right: $F < 1, P(H_0|D) = .82$).

The whole-brain analysis revealed three significant clusters sensitive to differences between real and CG faces (Fig. 5). In line with our ROI analysis, real as compared with CG faces elicited a significant activation cluster in the left FG. In addition, we observed significant opposite activation clusters (greater activations for CG vs. real faces) in the gyrus rectus and in the left nucleus accumbens. Table 3 presents a complete summary of significant activation clusters for all planned contrasts (Q1-Q4) in the whole-brain analysis.

3.2. Emotion effects

In our second research question, we asked whether emotional expressions of real and CG faces would evoke different brain responses in the FFA or AMG. Fig. 6 illustrates ROI analysis results by facial expression and face type. The main effect of emotion (ANG + FEA > NTR) was significant both in the FFA (left: $F(1, 19) = 11.22, p = .004, \eta_p^2 = .40,$

Table 3

Activation clusters sensitive to planned contrasts in whole-brain analysis.

RQ ^a	Contrast	Side	MNI coordinates			T	N. voxels
			x	y	z		
Q1	REAL > CG						
	FG	L	-41	-48	-19	4.58	371
	CG > REAL						
	GRect	L	-8	57	-20	5.08	474
	NAcc	L	-9	6	-15	5.72	257
	Q2	ANG + FEA > NTR					
	MTG	R	56	-57	5	4.80	381
	LingG	R	26	-57	0	4.49	295
	FEA > ANG						
	CalcG	L	-14	-100	1	4.57	346
	IOG	L	-31	-80	-21	5.16	216
	REAL > CG × ANG + FEA > NTR						
	SFG	L	-27	43	42	4.65	325
Q3	AVT > DIR						
	IOG	L	-31	-95	-20	2.46	1062
	REAL > CG × DIR > AVT						
	ITG	R	53	-64	-6	4.47	273
	ITG/MTG	L	-57	-70	1	6.44	1482
Q4	DIR > AVT × ANG > FEA						
	pSTS	R	65	-54	3	4.53	336
	IOG	R	24	-97	-13	4.82	751
	IOG	L	-23	-95	-19	5.75	1965
	MFG	L	-43	53	12	4.96	556

Note. Activation clusters were thresholded at $p < .001$ with a minimum cluster size set according to an estimated cluster-level threshold of $p < .05$. FG – fusiform gyrus, GRect – gyrus rectus, NAcc – nucleus accumbens, MTG – middle temporal gyrus, LingG – lingual gyrus, CalcG – calcarine gyrus, IOG – inferior occipital gyrus, SFG – superior frontal gyrus, pSTS – posterior superior temporal sulcus, MFG – middle frontal gyrus, ITG – inferior temporal gyrus.

^a Research question.

$P(H_1|D) = .96$; right: $F(1, 19) = 6.70, p = .019, \eta_p^2 = .28, P(H_1|D) = .82$) and in the right AMG ($F(1, 19) = 8.45, p = .009, \eta_p^2 = .31, P(H_1|D) = .90$). Difference between real and CG faces in the FFA was greater for fearful as compared with angry facial expressions (REAL > CG × FEA > ANG; left: $F(1, 17) = 9.67, p = .006, \eta_p^2 = .36, P(H_1|D) = .93$; right: $F(1, 17) = 6.16, p = .024, \eta_p^2 = .27, P(H_1|D) = .79$). Emotional faces did not elicit different responses in real and CG faces (REAL > CG × ANG + FEA > NTR) either in the AMG (left and right: $F(1, 19) < 1, P(H_0|D) = .78$) or in the FFA (left: $F(1, 17) < 1, P(H_0|D) = .79$; right: $F(1, 17) < 1, P(H_0|D) = .73$). On the contrary, simple effect tests showed that emotional faces (ANG + FEA > NTR) evoked significant responses in the right AMG both in real ($F(1, 19) = 5.28, p = .033, \eta_p^2 = .22, P(H_1|D) = .72$) and in CG faces ($F(1,$

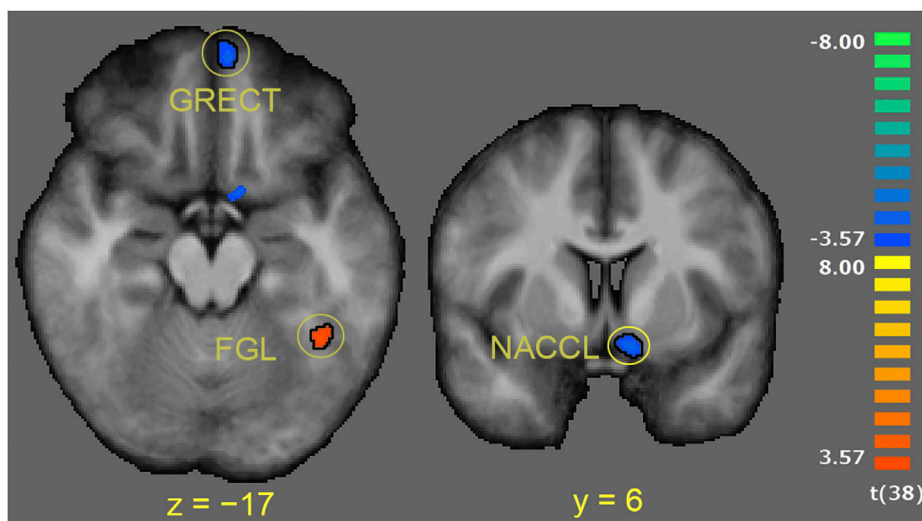


Fig. 5. Main effects of face type in whole-brain analysis: significantly greater activations to real vs. CG faces and to CG vs. real faces. GRECT – gyrus rectus, FG – fusiform gyrus, NACC – nucleus accumbens.

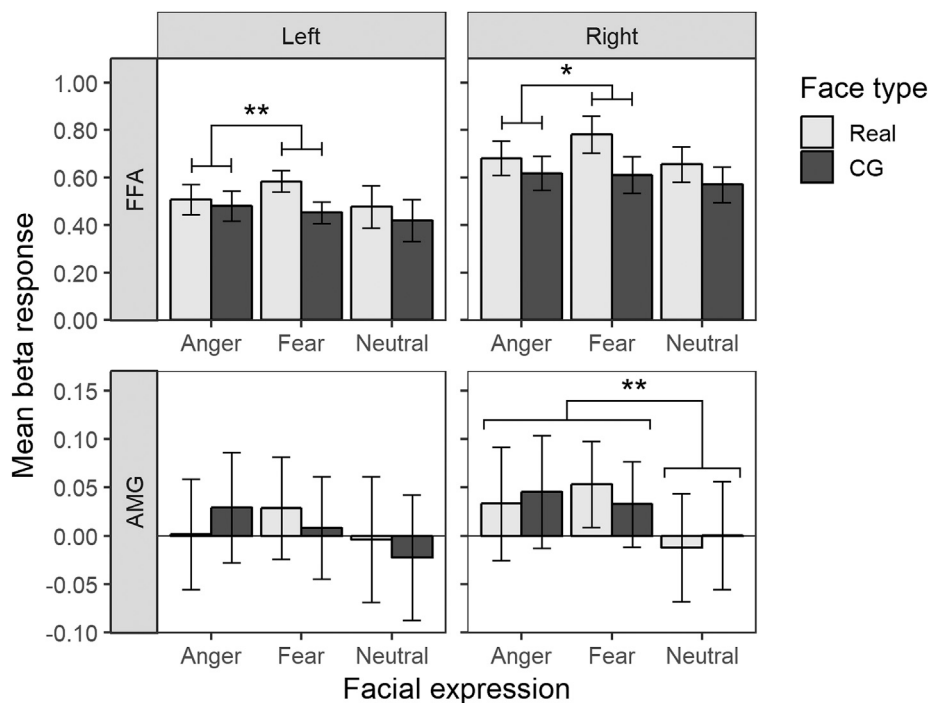


Fig. 6. Mean BOLD responses by facial expression and face type in the left and right fusiform face area (FFA) and amygdala (AMG). Error bars denote 95% CIs for difference between real and CG faces. Asterisks denote significant ($*p < .05$, $**p < .01$) planned contrasts for responses in the FFA (REAL > CG \times FEA > ANG) and AMG (ANG + FEA > NTR).

19) = 4.97, $p = .038$, $\eta_p^2 = .21$, $P(H_1|D) = .70$).

Whole-brain analysis showed that overall, emotional faces (ANG + FEA > NTR) and fearful as compared with angry faces (FEA > ANG) evoked significant activation clusters in occipital and temporal regions. Emotional faces evoked different responses in real as compared with CG faces (REAL > CG \times ANG + FEA > NTR) in the left superior frontal gyrus (SFG) (Table 3). Simple effect tests showed that emotional as compared with neutral facial expressions elicited greater activations in the SFG in real faces (M diff. = 0.12, $SE = 0.05$, $F(1, 19) = 5.36$, $p = .032$, $\eta_p^2 = .22$) but not in CG faces (M diff. = -0.12, $SE = 0.08$, $F(1, 19) = 2.51$, $p = .130$, $\eta_p^2 = .12$).

3.3. Gaze direction effects

In our third research question, we asked whether direct-gaze responses in the AMG would differ between real and CG faces. As illustrated in Fig. 7, ROI analysis showed that real faces evoked a significantly

greater direct-gaze response than CG faces (REAL > CG \times DIR > AVT) in the AMG (left: $F(1, 19) = 6.27$, $p = .022$, $\eta_p^2 = .25$, $P(H_1|D) = .79$; right: $F(1, 19) = 8.24$, $p = .010$, $\eta_p^2 = .30$, $P(H_1|D) = .89$). Simple effect tests showed that real faces with direct as compared with averted gaze evoked a greater response in the left AMG ($F(1, 19) = 6.48$, $p = .020$, $\eta_p^2 = .25$, $P(H_1|D) = .81$) and a similar albeit statistically non-significant response in the right AMG ($F(1, 19) = 4.11$, $p = .057$, $\eta_p^2 = .18$, $P(H_1|D) = .61$). We observed no evidence of gaze-related effects in CG faces (left: $F(1, 19) < 1$, $P(H_0|D) = .75$; right: $F(1, 19) = 1.87$, $p = .187$, $\eta_p^2 = .187$, $P(H_0|D) = .64$).

Whole-brain analysis showed that faces with averted as compared with direct gaze evoked one activation cluster in the left IOG, as shown in Fig. 8a. More importantly, responses to direct and averted gaze in the bilateral inferior temporal gyri (ITG) differed for real as compared with CG faces (REAL > CG \times DIR > AVT), as shown in Fig. 8b. Whereas in our ROI analysis the AMG responses were driven mainly by the direct gaze of real faces (Fig. 7), responses in the ITG were instead driven by the averted

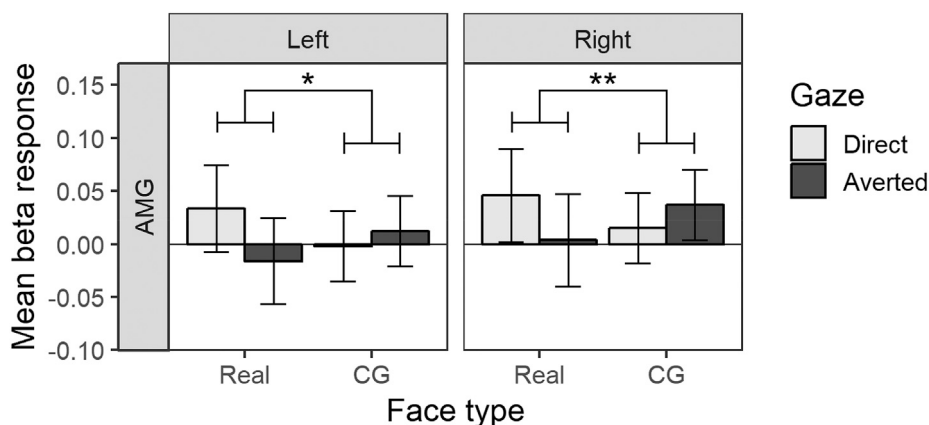


Fig. 7. Mean BOLD responses by face type and gaze direction in the left and right amygdala (AMG). Error bars denote 95% CIs for difference between direct and averted gaze. Asterisks denote significantly ($*p < .05$, $**p < .01$) different gaze effects for real and CG faces (REAL > CG \times DIR > AVT).

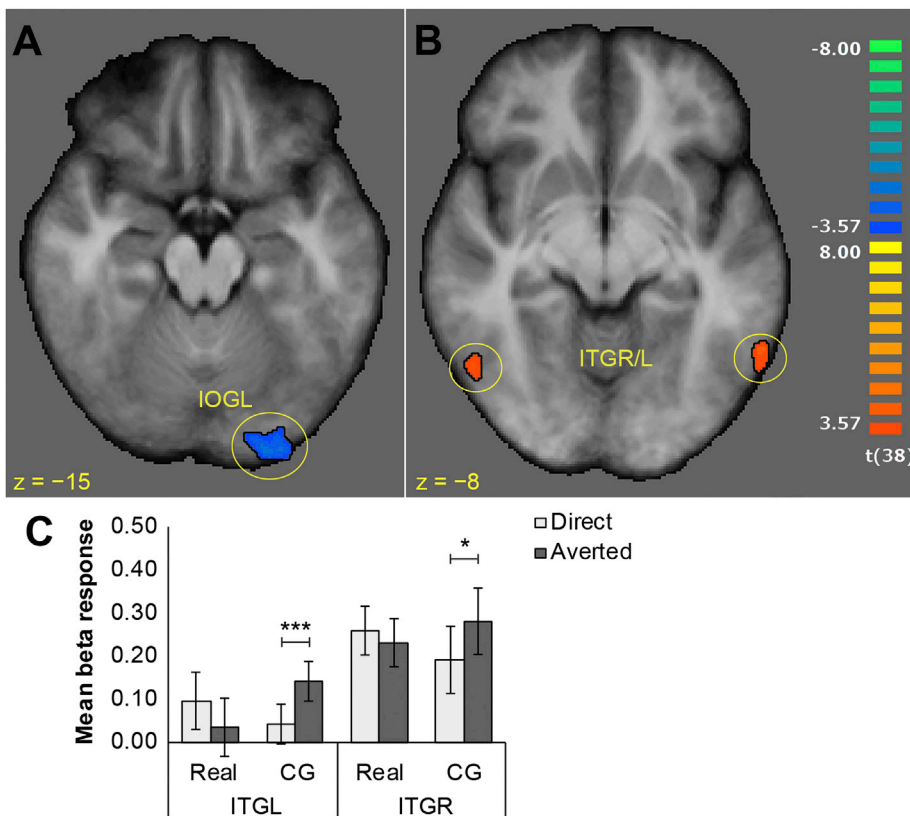


Fig. 8. Direct-gaze effects in the whole-brain analysis. a) Statistically significant activation clusters for averted vs. direct gaze. b) Significant activation clusters for interaction between face type (real vs. CG) and gaze direction (direct vs. averted). c) Parameter estimates for activation clusters sensitive to the interaction between face type and gaze direction. Error bars denote 95% CIs for the difference between direct and averted gaze, and asterisks denote statistically significant differences (* $p < .05$, *** $p < .001$).

gaze of CG faces (Fig. 8c). Specifically, simple effect tests showed that averted gaze evoked stronger responses than direct gaze in CG faces (left ITG: M diff. = 0.10, $SE = 0.02$, $F(1, 19) = 18.51$, $p < .001$, $\eta_p^2 = .49$; right ITG: M diff. = 0.09, $SE = 0.04$, $F(1, 19) = 5.54$, $p = .030$, $\eta_p^2 = .23$) but not in real faces (left ITG: M diff. = -0.06 , $SE = 0.03$, $F(1, 19) = 3.53$, $p = .076$, $\eta_p^2 = .16$; right ITG: M diff. = 0.03, $SE = 0.03$, $F(1, 19) = 1.05$, $p = .317$, $\eta_p^2 = .05$).

3.4. Shared signal effects

Our fourth research question was whether the interaction between gaze and facial expression – that is, the shared signal effect – would differ between real and CG faces. Fig. 9 illustrates AMG responses by gaze direction and facial expression. Region-of-interest analysis for the AMG did not provide support for the shared signal effect ($DIR > AVT \times ANG > FEA$; left: $F < 1$, $P(H_0|D) = .75$; right: $F < 1$, $P(H_0|D) = .81$) or its modulation by real and CG faces ($REAL > CG \times DIR > AVT \times ANG > FEA$; left and right: $F < 1$, $P(H_0|D) = .82$). As suggested by the Bayesian posterior probabilities, null hypothesis was more probable than either of these effects (i.e., $P(H_0|D) \geq .75$).

Importantly, the whole-brain analysis revealed significant activation clusters for the shared signal effect ($DIR > AVT \times ANG > FEA$) in the right pSTS, bilateral occipital regions (IOG extending to the lingual gyri), and left middle frontal gyrus (Fig. 10a). Activation patterns in these regions were clearly consistent with the shared signal hypothesis (Fig. 10b). Whole-brain analysis did not reveal any statistically significant activation clusters for shared signal effect differences between real and CG faces ($REAL > CG \times DIR > AVT \times ANG > FEA$).

4. Discussion

The present findings make several contributions to understanding how the brain encodes social information conveyed by realistic CG faces as opposed to real human faces. First, our results provide new evidence

on the similarities and differences in the neural encoding of real and artificial faces. Previous studies have provided inconsistent findings on whether real and artificial faces evoke different responses in core face processing regions. Our results showed that the FFA is able to detect such differences even for the CG faces used here, which are arguably much more realistic stimuli than for example previously employed cartoon faces (e.g., James et al., 2015; Tong et al., 2000). One possibility is that because CG faces tend to lack skin wrinkles and other fine-grained details, weaker FFA responses were related to its sensitivity to high spatial frequency information (Vuilleumier et al., 2003). The difference between real and CG faces was the greatest for fear, possibly because the horizontal stretching of the mouth in a fearful facial configuration is particularly difficult to model in CG faces. Second, despite the differential processing in the FFA, our findings demonstrate that the processing of emotional information (i.e., angry and fearful facial expressions) from real and CG faces again converges in the AMG, with no differences in activity between the two face types. This suggests that CG faces can evoke emotional processing in the brain that is similar to real faces. Our results hence replicate the previous findings of Moser et al. (2007); however, our results also significantly expand upon this study by considering AMG responses to specific emotions, direct and averted gaze, and the interaction between gaze and emotion. Our findings do not support the suggestion that near-human CG faces would evoke threat-related responses in the AMG, which would reflect potential aversive reactions as predicted by the uncanny valley hypothesis (Mori, 1970/2012).

Third, we extend previous findings on direct-gaze processing in the AMG (Brothers and Ring, 1993; Burra et al., 2013; Kawashima et al., 1999; Wicker et al., 2003) by demonstrating that the AMG is sensitive to direct gaze only in real and not in CG faces. We suggest that unlike CG faces, real faces are perceived as depicting social and intentional agents that are capable of focusing their attention on the observer. Hence, our results may have reflected the greater salience of direct gaze in alive as compared with inanimate faces. Our other fMRI findings did not, however, provide support for activations in animacy or mentalizing related

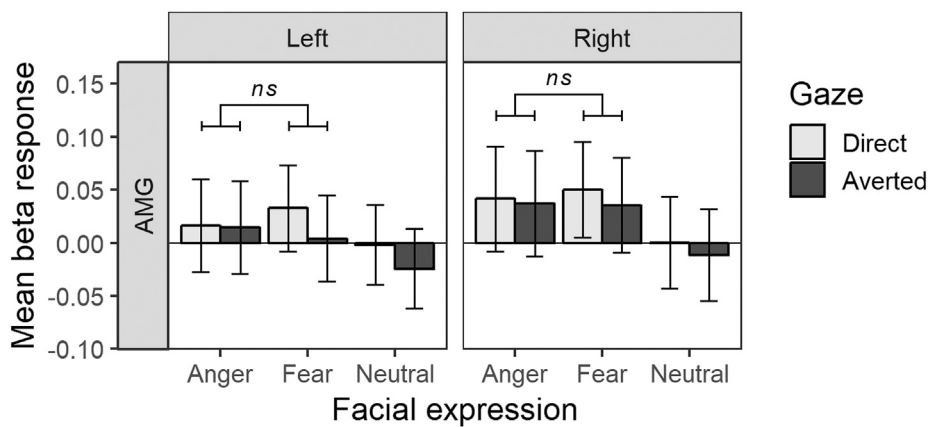


Fig. 9. Mean BOLD responses by facial expression and gaze direction in the left and right amygdala (AMG). Error bars denote 95% CIs for difference between direct and averted gaze. Non-significant contrasts (“ns”) for the shared signal effect are illustrated on the figure.

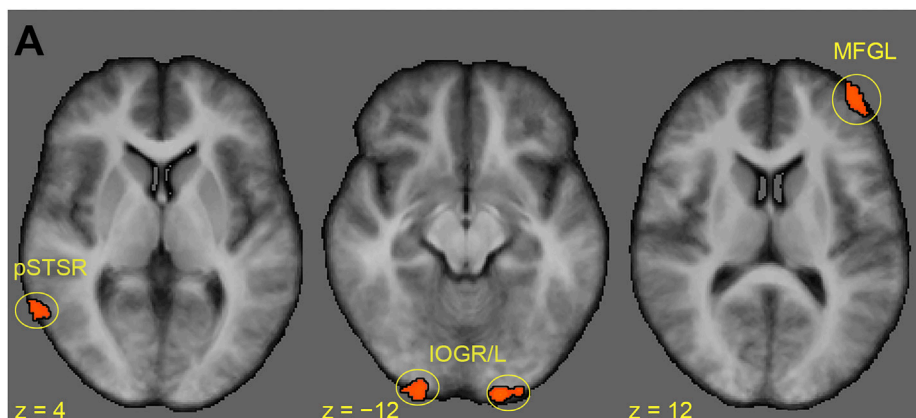
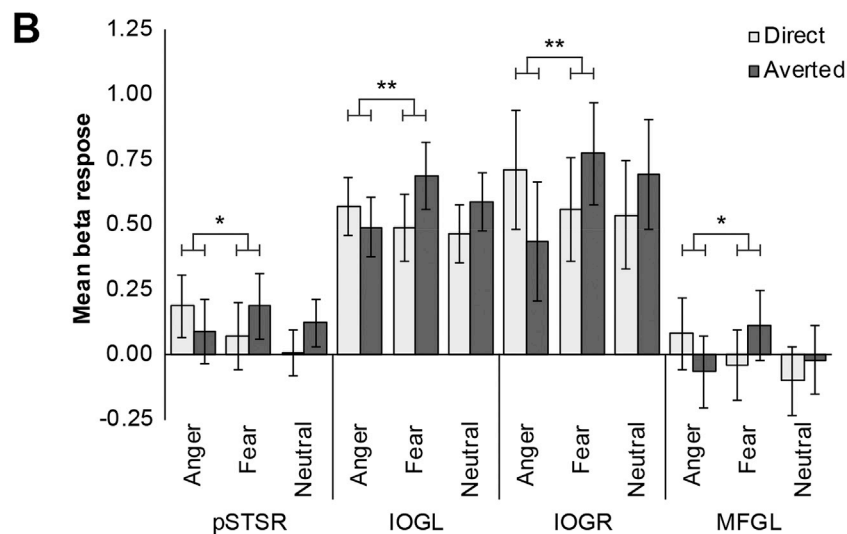


Fig. 10. Shared signal effects in the whole-brain analysis. a) Modulation of direct vs. averted gaze by angry vs. fearful faces (the shared signal effect). b) Parameter estimates for activation clusters sensitive to the shared signal effect. Error bars denote 95% confidence intervals for the difference between direct and averted gaze, and asterisks emphasize statistically significant contrasts for the shared signal effect (* $p < .05$, ** $p < .01$). pSTS – posterior superior temporal sulcus, IOG – inferior occipital gyrus, MFG – middle frontal gyrus.



networks. Alternatively, it is possible that the present findings could have been caused by subtle visual differences in the eye region. Even though the eye region of real and CG faces was matched carefully for luminosity and contrast, it is still possible that some local changes caused by gaze direction shifts (e.g., scleral reflections) were not modeled with sufficient fidelity in our CG faces. This issue could not have affected real faces, given that their averted gaze eye region was based on real photographs. This issue could also possibly explain why activations in some visual regions of the inferior and medial temporal cortex were driven mainly by

averted-gaze CG faces.

Fourth, our findings replicate shared signal responses in some regions that have been reported previously with CG faces, namely, the right pSTS, bilateral IOG, and MFG (N'Diaye et al., 2009). Given that these previous results were obtained using CG faces and we did not observe evidence for differences between real and CG faces, this suggests that CG and real faces may evoke similar shared signal responses in these regions. Previous neuroimaging evidence gives reason to believe that the IOG contributes primarily to low-level visual analysis of facial features

(Haxby et al., 2000; Ishai et al., 2005), whereas the MFG may play a role in the integration of “what” (e.g., facial feature analysis) and “where” (e.g., locus of attention) information from ventral and dorsal visual streams (de Borst et al., 2012; Japee et al., 2015). Furthermore, as supported by some previous EEG evidence (El Zein et al., 2015), the pSTS may respond differently to gaze direction depending on the facial expression. It is also conceivable that the pSTS could be involved in higher-order processes related to the shared signal effect (e.g., implicitly deciphering the source of threat), given that according to some theorists, the pSTS and its adjacent temporo-parietal junction (TPJ) are involved in mentalizing (Gobbini and Haxby, 2007; Nummenmaa and Calder, 2009). Contrary to some previous studies using briefly displayed static faces or dynamic faces (Adams et al., 2012; N'Diaye et al., 2009; Sato et al., 2004; van der Zwaag et al., 2012), we did not observe shared signal responses in the AMG either with real or CG faces.

Somewhat unexpectedly, real as compared with CG faces evoked poorer performance in our implicit catch trial task. We interpret this effect in terms of an involuntary attentional response towards human faces, which constitute a highly familiar and well-learned category of visual objects. This involuntary attentional shift may have interfered with performance in the catch trial task, which required refraining a motor response until the participant observed the catch stimulus. The observed weaker activations for real faces in the striatum and orbito-frontal cortex, which have previously been implicated in prediction error learning and outcome value monitoring (Hare et al., 2008), could reflect less efficient recruitment of sensorimotor learning processes for real faces. Alternatively, the striatum may also have encoded how CG faces deviate from prototypical human faces, as previously suggested by Cheetham et al. (2011).

We note some limitations to the present study. First, whereas Moser et al. (2007) used CG faces that had lower emotional intensity than real faces, in our study anger and fear were actually recognized better and anger was rated more intense when posed by CG faces. Even though these differences were relatively small (e.g., for intensity ratings, at most 14 points difference [upper 95% CL] on the 100-step scale), it is nevertheless possible that they might have compensated for otherwise weaker emotional responses to the CG faces. Importantly, we did not observe any fMRI effects that would have paralleled the greater intensity of angry or fearful CG facial expressions, however. Another potential limitation is that we used static images depicting intense facial emotions. For example, N'Diaye et al. (2009) used dynamic facial expressions and showed that the shared signal response in the AMG only occurs for facial expressions with weak intensity. Similarly, it has been shown that weak facial expressions elicit stronger behavioral responses to the shared signal effect (El Zein et al., 2015). These findings suggest that dynamic modality and uncertainty (i.e., weaker intensity) would strengthen the shared signal response in the AMG. It should be noted, however, that the shared signal response in the AMG has also been demonstrated with similar stimuli as we used in our study, that is, briefly displayed static images that depict intense facial expressions (Adams et al., 2012; van der Zwaag et al., 2012).

It is also possible that shared signal responses in the AMG would depend on the experimental task. Previous studies that have successfully demonstrated this effect have employed both passive viewing (e.g., Adams et al., 2012) and explicit (emotion intensity ratings in N'Diaye et al., 2009) and implicit (gender categorization in Sato et al., 2004) emotion recognition tasks. Our catch-trial task could possibly have drawn more attention away from the actual face stimuli than any of these tasks; however, we consider this possibility somewhat far-fetched given that catch-trial tasks have been used successfully in previous fMRI studies (e.g., Poyo Solanas et al., 2018). Methodologically, the present study also had a more complex design and, conversely, fewer repetitions per experimental condition than many previous shared signal studies which have employed a simple AB block design (e.g., Hadjikhani et al., 2008). Finally, we note that any study investigating artificial stimuli has to face the problem that “artificiality” does not have an unequivocal definition

or operationalization. We attempted to tackle this problem by using CG faces that were representative of typical CG faces that are accessible to behavioral and neuroscientists and by matching our CG and real face stimuli to the extent possible.

Taken together, the present study implies various similarities and differences in the neural encoding of social signals from real and CG faces. Although the overall processing of real and CG faces diverges in the FFA, the processing of emotional information from these face types seems to again converge in the AMG. In contrast, direct as compared with averted gaze evokes stronger responses in the AMG only in real and not in CG faces, which suggests caution in employing CG stimuli when investigating neural responses to social signals. In general, at least with static displays of intense facial emotions, interaction between gaze and emotion (i.e., the shared signal effect) activates specific clusters in the frontal and occipital cortex and in the pSTS, but not in the AMG. This study did not provide evidence for different shared signal responses in real and CG faces.

Conflicts of interest

The authors declare that they have no competing interests.

Acknowledgments

This project has received funding from the European Union's Horizon 2020 research and innovation programme under the Marie Skłodowska-Curie grant agreement No 703493 “NeuroBukimi” to JK, and from the European Research Council (ERC) under the European Union's seventh Framework Programme (FP/2007–2013) grant agreement No 295673 “EMOBODIES”. We would like to thank BICT Richard Benning, Maastricht University, Instrumentation Department, for his help in producing the computer-generated faces used in the present experiment.

Appendix

Data and analysis files are available from OSF: <https://osf.io/jqfbx>.

References

- Adams, R.B., Kleck, R.E., 2003. Perceived gaze direction and the processing of facial displays of emotion. *Psychol. Sci.* 14 (6), 644–647. <https://doi.org/10.1046/j.0956-7976.2003.psci.1479.x>.
- Adams Jr., R.B., Kleck, R.E., 2005. Effects of direct and averted gaze on the perception of facially communicated emotion. *Emotion* 5 (1), 3–11. <https://doi.org/10.1037/1528-3542.5.1.3>.
- Adams, R.B., Gordon, H.L., Baird, A.A., Ambady, N., Kleck, R.E., 2003. Effects of gaze on amygdala sensitivity to anger and fear faces. *Science* 300 (5625). <https://doi.org/10.1126/science.1082244>, 1536–1536.
- Adams, R.B., Franklin, R.G., Kveraga, K., Ambady, N., Kleck, R.E., Whalen, P.J., Nelson, A.J., 2012. Amygdala responses to averted vs direct gaze fear vary as a function of presentation speed. *Soc. Cogn. Affect. Neurosci.* 7 (5), 568–577. <https://doi.org/10.1093/scan/nsr038>.
- Bindemann, M., Mike Burton, A., Langton, S.R.H., 2008. How do eye gaze and facial expression interact? *Vis. Cogn.* 16 (6), 708–733. <https://doi.org/10.1080/13506280701269318>.
- de Borst, A.W., Sack, A.T., Jansma, B.M., Esposito, F., de Martino, F., Valente, G., Formisano, E., 2012. Integration of “what” and “where” in frontal cortex during visual imagery of scenes. *Neuroimage* 60 (1), 47–58. <https://doi.org/10.1016/j.neuroimage.2011.12.005>.
- Brothers, L., Ring, B., 1993. Mesial temporal neurons in the macaque monkey with responses selective for aspects of social stimuli. *Behav. Brain Res.* 57 (1), 53–61. [https://doi.org/10.1016/0166-4328\(93\)90061-T](https://doi.org/10.1016/0166-4328(93)90061-T).
- Burra, N., Hervais-Adelman, A., Kerzel, D., Tamietto, M., de Gelder, B., Pegna, A.J., 2013. Amygdala activation for eye contact despite complete cortical blindness. *J. Neurosci.* 33 (25), 10483–10489. <https://doi.org/10.1523/JNEUROSCI.3994-12.2013>.
- Calder, A.J., Lawrence, A.D., Keane, J., Scott, S.K., Owen, A.M., Christoffels, I., Young, A.W., 2002. Reading the mind from eye gaze. *Neuropsychologia* 40 (8), 1129–1138. [https://doi.org/10.1016/S0028-3932\(02\)00008-8](https://doi.org/10.1016/S0028-3932(02)00008-8).
- Chaminade, T., Zecca, M., Blakemore, S.-J., Takanishi, A., Frith, C.D., Micera, S., Umiltà, M.A., 2010. Brain response to a humanoid robot in areas implicated in the perception of human emotional gestures. *PLoS One* 5 (7), e11577. <https://doi.org/10.1371/journal.pone.0011577>.

- Cheetham, M., Suter, P., Jäncke, L., 2011. The human likeness dimension of the “uncanny valley hypothesis”: behavioral and functional MRI findings. *Front. Hum. Neurosci.* 5 (126) <https://doi.org/10.3389/fnhum.2011.00126>.
- Costafreda, S.G., Brammer, M.J., David, A.S., Fu, C.H.Y., 2008. Predictors of amygdala activation during the processing of emotional stimuli: a meta-analysis of 385 PET and fMRI studies. *Brain Res. Rev.* 58 (1), 57–70. <https://doi.org/10.1016/j.brainresrev.2007.10.012>.
- Desikan, R.S., Ségonne, F., Fischl, B., Quinn, B.T., Dickerson, B.C., Blacker, D., Killiany, R.J., 2006. An automated labeling system for subdividing the human cerebral cortex on MRI scans into gyral based regions of interest. *Neuroimage* 31 (3), 968–980. <https://doi.org/10.1016/j.neuroimage.2006.01.021>.
- Dubal, S., Foucher, A., Jouvett, R., Nadel, J., 2011. Human brain spots emotion in non humanoid robots. *Soc. Cogn. Affect. Neurosci.* 6 (1), 90–97. <https://doi.org/10.1093/scan/nsq019>.
- Engelen, T., de Graaf, T.A., Sack, A.T., de Gelder, B., 2015. A causal role for inferior parietal lobule in emotion body perception. *Cortex* 73, 195–202. <https://doi.org/10.1016/j.cortex.2015.08.013>.
- Engell, A.D., Haxby, J.V., 2007. Facial expression and gaze-direction in human superior temporal sulcus. *Neuropsychologia* 45 (14), 3234–3241. <https://doi.org/10.1016/j.neuropsychologia.2007.06.022>.
- Farid, H., Bravo, M.J., 2012. Perceptual discrimination of computer generated and photographic faces. *Digit. Invest.* 8 (3), 226–235. <https://doi.org/10.1016/j.diin.2011.06.003>.
- Fonov, V., Evans, A.C., Botteron, K., Almli, C.R., McKinstry, R.C., Collins, D.L., 2011. Unbiased average age-appropriate atlases for pediatric studies. *Neuroimage* 54 (1), 313–327. <https://doi.org/10.1016/j.neuroimage.2010.07.033>.
- Fox, C.J., Iaria, G., Barton, J.J.S., 2009. Defining the face processing network: optimization of the functional localizer in fMRI. *Hum. Brain Mapp.* 30 (5), 1637–1651. <https://doi.org/10.1002/hbm.20630>.
- Fusar-Poli, P., Placentino, A., Carletti, F., Landi, P., Allen, P., Surguladze, S., Politi, P., 2009. Functional atlas of emotional faces processing: a voxel-based meta-analysis of 105 functional magnetic resonance imaging studies. *J. Psychiatry Neurosci.* 34 (6), 418.
- de Gelder, B., Rouw, R., 2001. Beyond localisation: a dynamical dual route account of face recognition. *Acta Psychol.* 107 (1–3), 183–207. [https://doi.org/10.1016/s0001-6918\(01\)00024-5](https://doi.org/10.1016/s0001-6918(01)00024-5).
- Gobbini, M.I., Haxby, J.V., 2007. Neural systems for recognition of familiar faces. *Neuropsychologia* 45 (1), 32–41. <https://doi.org/10.1016/j.neuropsychologia.2006.04.015>.
- Gobbini, M.I., Gentili, C., Ricciardi, E., Bellucci, C., Salvini, P., Laschi, C., Pietrini, P., 2011. Distinct neural systems involved in agency and animacy detection. *J. Cogn. Neurosci.* 23 (8), 1911–1920. <https://doi.org/10.1162/jocn.2010.21574>.
- Goebel, R., Esposito, F., Formisano, E., 2006. Analysis of functional image analysis contest (FIAC) data with BrainVoyager QX: from single-subject to cortically aligned group general linear model analysis and self-organizing group independent component analysis. *Hum. Brain Mapp.* 27 (5), 392–401. <https://doi.org/10.1002/hbm.20249>.
- Hadjikhani, N., Hoge, R., Snyder, J., de Gelder, B., 2008. Pointing with the eyes: the role of gaze in communicating danger. *Brain Cogn.* 68 (1), 1–8. <https://doi.org/10.1016/j.bandc.2008.01.008>.
- Hare, T.A., O’Doherty, J., Camerer, C.F., Schultz, W., Rangel, A., 2008. Dissociating the role of the orbitofrontal cortex and the striatum in the computation of goal values and prediction errors. *J. Neurosci.* 28 (22), 5623–5630. <https://doi.org/10.1523/JNEUROSCI.1309-08.2008>.
- Haxby, J.V., Hoffman, E.A., Gobbini, M.I., 2000. The distributed human neural system for face perception. *Trends Cogn. Sci.* 4 (6), 223–233. [https://doi.org/10.1016/S1364-6613\(00\)01482-0](https://doi.org/10.1016/S1364-6613(00)01482-0).
- Iidaka, T., 2014. Role of the fusiform gyrus and superior temporal sulcus in face perception and recognition: an empirical review. *Jpn. Psychol. Res.* 56 (1), 33–45. <https://doi.org/10.1111/jpr.12018>.
- Ishai, A., 2008. Let’s face it: it’s a cortical network. *Neuroimage* 40 (2), 415–419. <https://doi.org/10.1016/j.neuroimage.2007.10.040>.
- Ishai, A., Schmidt, C.F., Boesiger, P., 2005. Face perception is mediated by a distributed cortical network. *Brain Res. Bull.* 67 (1–2), 87–93. <https://doi.org/10.1016/j.brainresbull.2005.05.027>.
- Jack, R.E., Garrod, O.G.B., Yu, H., Caldara, R., Schyns, P.G., 2012. Facial expressions of emotion are not culturally universal. *Proc. Natl. Acad. Sci.* 109 (19), 7241–7244. <https://doi.org/10.1073/pnas.1200155109>.
- James, T.W., Potter, R.F., Lee, S., Kim, S., Stevenson, R.A., Lang, A., 2015. How realistic should avatars be? An initial fMRI investigation of activation of the face perception network by real and animated faces. *J. Media Psychol.: Theor. Methods Appl.* 27 (3), 109–117. <https://doi.org/10.1027/1864-1105/a000156>.
- Japee, S., Holiday, K., Satyshur, M.D., Mukai, I., Ungerleider, L.G., 2015. A role of right middle frontal gyrus in reorienting of attention: a case study. *Front. Syst. Neurosci.* 9, 23. <https://doi.org/10.3389/fnsys.2015.00023>.
- Jiang, F., Dricot, L., Blanz, V., Goebel, R., Rossion, B., 2009. Neural correlates of shape and surface reflectance information in individual faces. *Neuroscience* 163 (4), 1078–1091. <https://doi.org/10.1016/j.neuroscience.2009.07.062>.
- Johnson, M.H., 2005. Subcortical face processing. *Nat. Rev. Neurosci.* 6 (10), 766–774. <https://doi.org/10.1038/nrn1766>.
- Joyal, C.C., 2014. Virtual faces expressing emotions: an initial concomitant and construct validity study. *Front. Hum. Neurosci.* 8, 787. <https://doi.org/10.3389/fnhum.2014.00787>.
- Kawabata Duncan, K.J., Devlin, J.T., 2011. Improving the reliability of functional localizers. *Neuroimage* 57 (3), 1022–1030. <https://doi.org/10.1016/j.neuroimage.2011.05.009>.
- Kawashima, R., Sugiura, M., Kato, T., Nakamura, A., Hatano, K., Ito, K., Nakamura, K., 1999. The human amygdala plays an important role in gaze monitoring: a PET study. *Brain* 122 (4), 779–783. <https://doi.org/10.1093/brain/122.4.779>.
- Langner, O., Dotsch, R., Bijlstra, G., Wigboldus, D.H.J., Hawk, S.T., van Knippenberg, A., 2010. Presentation and validation of the Radboud faces database. *Cognit. Emot.* 24 (8), 1377–1388. <https://doi.org/10.1080/02699930903485076>.
- Masson, M.E.J., 2011. A tutorial on a practical Bayesian alternative to null-hypothesis significance testing. *Behav. Res. Methods* 43 (3), 679–690. <https://doi.org/10.3758/s13428-010-0049-5>.
- Mattavelli, G., Sormaz, M., Flack, T., Asghar, A.U.R., Fan, S., Frey, J., Andrews, T.J., 2014. Neural responses to facial expressions support the role of the amygdala in processing threat. *Soc. Cogn. Affect. Neurosci.* 9 (11), 1684–1689. <https://doi.org/10.1093/scan/nst162>.
- Mori, M., 1970/2012. The uncanny valley (K. F. MacDorman & N. Kageki, trans.). *IEEE Robot. Autom. Mag.* 19 (2), 98–100. <https://doi.org/10.1109/MRA.2012.2192811>.
- Moser, E., Derntl, B., Robinson, S., Fink, B., Gur, R.C., Grammer, K., 2007. Amygdala activation at 3T in response to human and avatar facial expressions of emotions. *J. Neurosci. Methods* 161 (1), 126–133. <https://doi.org/10.1016/j.jneumeth.2006.10.016>.
- Nummenmaa, L., Calder, A.J., 2009. Neural mechanisms of social attention. *Trends Cogn. Sci.* 13 (3), 135–143. <https://doi.org/10.1016/j.tics.2008.12.006>.
- N’Diaye, K., Sander, D., Vuilleumier, P., 2009. Self-relevance processing in the human amygdala: gaze direction, facial expression, and emotion intensity. *Emotion* 9 (6), 798–806. <https://doi.org/10.1037/a0017845>.
- Pönkänen, L.M., Alhoniemi, A., Leppänen, J.M., Hietanen, J.K., 2011. Does it make a difference if I have an eye contact with you or with your picture? An ERP study. *Soc. Cogn. Affect. Neurosci.* 6 (4), 486–494. <https://doi.org/10.1093/scan/nsq068>.
- Poyo Solanas, M., Zhan, M., Vaessen, M., Hortensius, R., Engelen, T., de Gelder, B., 2018. Looking at the face and seeing the whole body. Neural basis of combined face and body expressions. *Soc. Cogn. Affect. Neurosci.* 13 (1), 135–144. <https://doi.org/10.1093/scan/nsx130>.
- Raffery, A.E., 1999. Bayes factors and BIC: comment on “A critique of the Bayesian information criterion for model selection. *Sociol. Methods Res.* 27, 411–427. <https://doi.org/10.1177/0049124199027003005>.
- Ramon, M., Dricot, L., Rossion, B., 2010. Personally familiar faces are perceived categorically in face-selective regions other than the fusiform face area: response properties of face-preferential regions. *Eur. J. Neurosci.* 32 (9), 1587–1598. <https://doi.org/10.1111/j.1460-9568.2010.07405.x>.
- Rossion, B., Hanseeuw, B., Dricot, L., 2012. Defining face perception areas in the human brain: a large-scale factorial fMRI face localizer analysis. *Brain Cogn.* 79 (2), 138–157. <https://doi.org/10.1016/j.bandc.2012.01.001>.
- Said, C.P., 2010. Graded representations of emotional expressions in the left superior temporal sulcus. *Front. Syst. Neurosci.* 4 <https://doi.org/10.3389/fnsys.2010.00006>.
- Sander, D., Grandjean, D., Kaiser, S., Wehrle, T., Scherer, K.R., 2007. Interaction effects of perceived gaze direction and dynamic facial expression: evidence for appraisal theories of emotion. *Eur. J. Cogn. Psychol.* 19 (3), 470–480. <https://doi.org/10.1080/09541440600757426>.
- Sato, W., Yoshikawa, S., Kochiyama, T., Matsumura, M., 2004. The amygdala processes the emotional significance of facial expressions: an fMRI investigation using the interaction between expression and face direction. *Neuroimage* 22 (2), 1006–1013. <https://doi.org/10.1016/j.neuroimage.2004.02.030>.
- Sauer, A., Mothes-Lasch, M., Miltner, W.H.R., Straube, T., 2014. Effects of gaze direction, head orientation and valence of facial expression on amygdala activity. *Soc. Cogn. Affect. Neurosci.* 9 (8), 1246–1252. <https://doi.org/10.1093/scan/nst100>.
- Schindler, S., Zell, E., Botsch, M., Kissler, J., 2017. Differential effects of face-realism and emotion on event-related brain potentials and their implications for the uncanny valley theory. *Sci. Rep.* 7 (1) <https://doi.org/10.1038/srep45003>.
- Schultz, J., Pilz, K.S., 2009. Natural facial motion enhances cortical responses to faces. *Exp. Brain Res.* 194 (3), 465–475. <https://doi.org/10.1007/s00221-009-1721-9>.
- Senju, A., Johnson, M.H., 2009. The eye contact effect: mechanisms and development. *Trends Cogn. Sci.* 13 (3), 127–134. <https://doi.org/10.1016/j.tics.2008.11.009>.
- Straube, T., Langohr, B., Schmidt, S., Mentzel, H.-J., Miltner, W.H.R., 2010. Increased amygdala activation to averted versus direct gaze in humans is independent of valence of facial expression. *Neuroimage* 49 (3), 2680–2686. <https://doi.org/10.1016/j.neuroimage.2009.10.074>.
- Tamietto, M., de Gelder, B., 2010. Neural bases of the non-conscious perception of emotional signals. *Nat. Rev. Neurosci.* 11 (10), 697–709. <https://doi.org/10.1038/nrn2889>.
- Tong, F., Nakayama, K., Moscovich, M., Weinrib, O., Kanwisher, N., 2000. Response properties of the human fusiform face area. *Cogn. Neuropsychol.* 17 (1–3), 257–280. <https://doi.org/10.1080/026432900380607>.
- Vuilleumier, P., Pourtois, G., 2007. Distributed and interactive brain mechanisms during emotion face perception: evidence from functional neuroimaging. *Neuropsychologia* 45 (1), 174–194. <https://doi.org/10.1016/j.neuropsychologia.2006.06.003>.
- Vuilleumier, P., Armony, J.L., Driver, J., Dolan, R.J., 2003. Distinct spatial frequency sensitivities for processing faces and emotional expressions. *Nat. Neurosci.* 6 (6), 624–631. <https://doi.org/10.1038/nrn1057>.
- Wagenmakers, E.-J., 2007. A practical solution to the pervasive problems of p values. *Psychon. Bull. Rev.* 14 (5), 779–804. <https://doi.org/10.3758/bf03194105>.
- Whalen, P.J., 2004. Human amygdala responsivity to masked fearful eye whites. *Science* 306 (5704). <https://doi.org/10.1126/science.1103617>, 2061–2061.
- Wicker, B., Michel, F., Henaff, M.-A., Decety, J., 1998. Brain regions involved in the perception of gaze: a PET study. *Neuroimage* 8 (2), 221–227. <https://doi.org/10.1006/nimg.1998.0357>.

- Wicker, B., Perrett, D.I., Baron-Cohen, S., Decety, J., 2003. Being the target of another's emotion: a PET study. *Neuropsychologia* 41 (2), 139–146. [https://doi.org/10.1016/S0028-3932\(02\)00144-6](https://doi.org/10.1016/S0028-3932(02)00144-6).
- Yarkoni, T., Poldrack, R.A., Nichols, T.E., Van Essen, D.C., Wager, T.D., 2011. Large-scale automated synthesis of human functional neuroimaging data. *Nat. Methods* 8 (8), 665–670. <https://doi.org/10.1038/nmeth.1635>.
- El Zein, M., Wyart, V., Grèzes, J., 2015. Anxiety dissociates the adaptive functions of sensory and motor response enhancements to social threats. *ELife* 4. <https://doi.org/10.7554/eLife.10274>.
- van der Zwaag, W., Da Costa, S.E., Zürcher, N.R., Adams, R.B., Hadjikhani, N., 2012. A 7 tesla fMRI study of amygdala responses to fearful faces. *Brain Topogr.* 25 (2), 125–128. <https://doi.org/10.1007/s10548-012-0219-0>.